



HAL
open science

First evaluation of the effect of microorganisms on steady state hydroxyl radical concentrations in atmospheric waters

A. Lallement, V. Vinatier, M. Brigante, Laurent Deguillaume, A.M. Delort, G. Mailhot

► To cite this version:

A. Lallement, V. Vinatier, M. Brigante, Laurent Deguillaume, A.M. Delort, et al.. First evaluation of the effect of microorganisms on steady state hydroxyl radical concentrations in atmospheric waters. *Chemosphere*, 2018, 212, pp.715 - 722. 10.1016/j.chemosphere.2018.08.128 . hal-01874247

HAL Id: hal-01874247

<https://hal.science/hal-01874247>

Submitted on 9 Dec 2020

HAL is a multi-disciplinary open access archive for the deposit and dissemination of scientific research documents, whether they are published or not. The documents may come from teaching and research institutions in France or abroad, or from public or private research centers.

L'archive ouverte pluridisciplinaire **HAL**, est destinée au dépôt et à la diffusion de documents scientifiques de niveau recherche, publiés ou non, émanant des établissements d'enseignement et de recherche français ou étrangers, des laboratoires publics ou privés.

1 **FIRST EVALUATION OF THE EFFECT OF MICROORGANISMS ON**
2 **STEADY STATE HYDROXYL RADICAL CONCENTRATIONS IN**
3 **ATMOSPHERIC WATERS**

4 **A. Lallement¹, V. Vinatier¹, M. Brigante¹, L. Deguillaume², A. M. Delort^{1*} and G.**
5 **Mailhot^{1*}**

6 ¹ Université Clermont Auvergne, CNRS, SIGMA Clermont, Institut de Chimie de Clermont-
7 Ferrand, 63000 Clermont-Ferrand, France

8 ² Université Clermont Auvergne, CNRS, Laboratoire de Météorologie Physique, 63000
9 Clermont-Ferrand, France

10
11 **Corresponding author: A-marie.Delort@uca.fr, gilles.mailhot@uca.fr*

12
13 **Abstract**

14 Clouds are complex multiphasic media where efficient chemical reactions take place and
15 where microorganisms have been found to be metabolically active. Hydroxyl radical is the
16 main oxidant in cloud water, and more generally in the atmosphere, during the day and drives
17 the cloud oxidative capacity. However, only one measurement of the steady state hydroxyl
18 radical concentrations in cloud water has been reported so far. Cloud chemistry models are
19 used to estimate the hydroxyl radical concentrations with values ranging from 10^{-12} to 10^{-15} M
20 that are surely overestimated due to a lack of knowledge about the speciation of the organic
21 matter acting as a sink for hydroxyl radicals. The aim of this work is to quantify the
22 concentration of hydroxyl radicals at steady state in rain and cloud waters and to measure the
23 impact of native microflora on this concentration. First, the non-toxicity of terephthalic acid
24 as probe is controlled before the analysis in real atmospheric water samples. Higher

25 concentrations of hydroxyl radicals are found in cloud waters than in rain waters, with a mean
26 value " 1.6 ± 1.5 " $\times 10^{-16}$ M and " 7.2 ± 5.0 " $\times 10^{-16}$ M for rain and cloud waters respectively
27 and no real impact of microorganisms was observed. This method allows the measurement of
28 steady state hydroxyl radical levels at very low concentrations (down to 10^{-17} M) and it is
29 biocompatible, fast and easy to handle. It is a useful tool, complementary to other methods, to
30 give a better overview of atmospheric water oxidant capacity.

31

32 **Keywords**

33 Cloud water, photochemistry, radical chemistry, oxidative capacity, microorganisms
34 interaction.

35

36 **1. Introduction**

37 Clouds are multiphasic systems where many chemical reactions occur, particularly in droplets
38 (Faust, 1994; Herrmann et al., 2015; Lelieveld and Crutzen, 1991). Very efficient
39 photochemical processes take place inside droplets and chemical reactions within clouds can
40 be faster than the equivalent reactions in the gas phase. The aqueous phase chemistry leads to
41 oxidation processes that can be driven by reactions with radicals. Among the radicals,
42 hydroxyl radical is the most efficient oxidant in the atmosphere (Lelieveld et al., 2004).
43 Several works were carried out on hydroxyl radical chemistry in cloud to define $\bullet\text{OH}$ sources
44 and reactivity (Blough and Zepp, 1995; Chameides and Davis, 1982; Jacob, 1986; Mauldin III
45 et al., 1997). Main sources of hydroxyl radical are i) hydrogen peroxide, nitrite and nitrate
46 photolysis (Yu and Barker, 2003; Zafiriou and Bonneau, 1987; Zellner et al., 1990; Zepp et
47 al., 1987), ii) iron *via* ligand-to-metal charge-transfer reactions or photo-Fenton chemistry
48 (Deguillaume et al., 2004, 2005; Faust and Hoigné, 1990; Faust and Zepp, 1993; Nakatani et
49 al., 2007; Weschler et al., 1986), iii) the reaction of ozone towards the superoxide radicals and

50 iv) the mass transfer of $\bullet\text{OH}$ from the gas phase to the aqueous phase (Arakaki and Faust,
51 1998; Faust and Allen, 1993). In terms of $\bullet\text{OH}$ sinks, the main way is the reactivity with
52 dissolved organic matter (Arakaki et al., 2013). However, due to the complexity of this
53 environmental matrix, the organic composition is poorly characterized (Herckes et al., 2013);
54 for example, only 21% of the organic matter in cloud waters sampled at the puy de Dôme
55 station is characterized (Bianco et al., 2016). Furthermore, microorganisms are also present
56 and metabolically active in cloud water. They can survive in spite of numerous stress factors
57 like osmotic shocks, temperature changes and freeze-thaw cycles (Amato et al., 2007a; Joly et
58 al., 2015). In order to survive, they use organic matter as a source of carbon such as short
59 chain aldehydes and carboxylic acids (Amato et al., 2007b; Ariya et al., 2002; Vaitilingom et
60 al., 2011) but they also have an effect on the oxygenated compounds. As aerobic cells, they
61 are able to consume or either neutralize Reactive Oxygen Species (ROS) like hydroxyl
62 radical, singlet oxygen and hydrogen peroxide. Cloud microorganisms, present in cloud water,
63 have the capacity to degrade hydrogen peroxide and can contribute to the degradation of
64 organic compounds during the day and even more during the night (Vaitilingom et al., 2010,
65 2013).

66 Up to now, the hydroxyl radical concentrations have been estimated using cloud chemistry
67 models. These models consider multiphase chemistry and the mass transfer from the gas to
68 the aqueous phase. Simulated concentrations range from 10^{-12} to 10^{-15} M (Deguillaume et al.,
69 2004, 2005, Herrmann et al., 2000, 2010; Mouchel-Vallon et al., 2017; Tilgner and Herrmann,
70 2010; Tilgner et al., 2013) depending on the chemical scenarios and on the complexity of the
71 chemical mechanisms. For example, the amounts of organic matter and iron are key
72 parameters that drive the level of $\bullet\text{OH}$. Moreover, formation rates of hydroxyl radical in
73 irradiated rain or cloud waters are measured in the laboratory (Faust and Allen, 1993;
74 Nakatani et al., 2007) and are used to evaluate cloud chemistry models (Bianco et al., 2015);

75 they express the maximum of $\bullet\text{OH}$ concentration formed without taking into account the
76 different scavengers present in cloud water. The steady state hydroxyl radical concentrations
77 have been estimated in different surface waters (Arakaki et al., 1999; Brezonik and Fulkerson-
78 Brekken, 1998; Haag and Hoigné, 1985; al Housari et al., 2010; Mill et al., 1980; Qian et al.,
79 2001; Russi et al., 1982; Zepp et al., 1987; Zhou and Mopper, 1990) but, to our knowledge,
80 the study of Anastasio and McGregor (2001) is the only one on cloud water. In their
81 experiments, they used benzene and benzoic acid as chemical probes at concentrations
82 ranging from 50 to 1500 μM and analyzed reaction products by HPLC. Because the most
83 concentrated species in cloud water are in the μM range, addition of a probe in high
84 concentration can impact the biological activity which is controlled by the environment
85 (Metallo and Vander Heiden, 2013; Shingler, 2003; Tropel and Meer, 2004). Toxicity issues
86 could also arise. Existing methods must then be adapted to study the impact of
87 microorganisms. Moreover to take biological variability into account several experiments
88 must be performed in parallel with strictly identical conditions.

89 The main goal of our study is to evaluate the stationary concentration of OH radicals in
90 atmospheric waters and the potential impact of microorganisms on this concentration. For that
91 purpose we had to develop a specific method which main characteristics are i) to take into
92 account the native microorganisms, and their viability, ii) the use of small volume of sample
93 (300 μL /well) for one measurement so 6 mL for a complete analysis, and iii) the direct and
94 fast measurement by fluorescence, without chromatography technics.

95

96 **2. Experimental section**

97

98 *2.1. Chemicals*

99 Terephthalic acid (TA) (Sigma Aldrich) and 2-hydroxyterephthalic acid (TAOH) (Atlantic
100 Research Chemical), with a purity of 98 and 97% respectively, are used without additional
101 purification. Acetic acid and H₂SO₄ are from Acros Organic. Formic acid, oxalic acid,
102 succinic acid, K₂SO₄, MgCl₂·6H₂O, NO₃NH₄, NaH₂PO₄·2H₂O, Na₂HPO₄·2H₂O, ferrozine and
103 hydrogen peroxide (30% in water, not stabilized) are from Fluka. CaCl₂·2H₂O, NaCl, horse
104 radish peroxydase, Tris-EDTA buffer solution, dimethylsulfoxide (DMSO), FeCl₃·6H₂O and
105 ethylenediamine-N,N'-disuccinic acid (EDDS) are from Sigma Aldrich. NaOH is from Merck
106 and 4-hydroxyphenylacetic acid is from Alfa Aesar®.

107

108 2.2. *Irradiation setup*

109 Lamps used for the irradiation setup are tropical terrarium bulb call Reptile UVB (13 W) from
110 Exo Terra®. The polychromatic emission spectrum of the irradiation system reaching the
111 solution is recorded using an optical fiber with a charge coupled device (CCD)
112 spectrophotometer (Ocean Optics USD 2000 + UV-vis) which is calibrated using a DH-2000-
113 CAL Deuterium Tungsten Halogen reference lamp. The total irradiance in the UV region of
114 solar spectrum (290 and 400 nm) reaching the solution is then estimated to be 915 μW cm⁻².
115 In Fig. 1, the lamp emission is compared with the solar spectrum measured at the puy de
116 Dôme station under cloudy or clear sky conditions.

117

118 2.3. *Sampling and analysis of natural atmospheric waters (cloud and rain)*

119 Rain samples were collected in September 17th, October 28th and December 2nd, 2015 and on
120 February 17th and September 15th, 2016 on OPGC (Observatoire de Physique du Globe de
121 Clermont-Ferrand) building roof (435 m above sea level, 45°76' North, 3°11' East, France)
122 with a homemade pluviometer, composed of sterilized Erlenmeyer flask (2 000 mL) and
123 sterilized funnel. Cloud waters were collected on February 16th, April 1st, June 1st and 5th and

124 July 2nd, 2016 at the puy de Dôme station (1 465 m above the sea level, 45°46' North, 2°57'
125 East, France) that belongs to the atmospheric survey networks EMEP (the European
126 Monitoring and Evaluation Program), GAW (Global Atmosphere Watch) and ACTRIS
127 (Aerosols, Clouds, and Trace gases Research Infrastructure). For this, a sterilized single-stage
128 cloud collector was used as described in Deguillaume et al. (2014).

129 Cloud and rain samples are kept in the dark and stored at 4°C before the experimentation.
130 Chemical composition analyses are performed on cloud and rain samples through pH, total
131 organic carbon (TOC) concentration, iron concentration and ionic species concentrations. The
132 pH is measured before and after experimentation with a pH meter MP 225 (Mettler Toledo).
133 TOC analyses are performed with TOC 5050A analyzer (Shimatzu). Concentrations of Fe(II)
134 and Fe(III) are quantified by spectrophotometric assays after complexation with ferrozine
135 (colorimetric complexing agent) as described by Parazols et al. (2007). Ionic species are
136 quantified by ion chromatography with a Dionex DX320 column for anions and a Dionex
137 ICS1500 column for cations. For microbiological characterization, cells are counted by flow
138 cytometry. Cultured microorganisms are grown on R2A medium at 5 and 17°C. ATP is
139 measured with BioThema[®] ATP Biomass kit HS.

140 Measurements of hydroxyl radical concentrations in atmospheric waters are performed under
141 irradiation and with filtered or non-filtered samples. Waters are filtered just before filling the
142 plate, thanks to a Minisart[®] PES filter (pore size of 0.22 µm and filter diameter of 28 mm
143 from Sartorius, Germany) under sterilized conditions.

144 All the vessels are washed with hydrochloric acid solution (2 M) and rinsed with ultrapure
145 water and then sterilized.

146

147 2.4. *Determination of steady state hydroxyl radical concentrations*

148 The detection of •OH radical is based on the reaction with TA (Fig. 2):

149 Among the products formed 2-Hydroxyterephthalic acid (TAOH) is detected and quantified
 150 due to its strong fluorescence. However, TAOH is not the unique byproduct and could be
 151 instable under irradiation (Page et al., 2010). For these reasons, TAOH formation yield
 152 (γ_{TAOH}) was previously described and evaluated as a function of irradiation conditions,
 153 temperature and pH by Charbouillot *et al.* (2011). In the same work the second order rate
 154 constant between TA and $\bullet\text{OH}$ was determined, $k_{TA} = "4.1 \pm 0.1" \times 10^9 \text{ M}^{-1} \text{ s}^{-1}$.

155 In order to obtain the real steady state concentration of $\bullet\text{OH}$ ($[\bullet\text{OH}]_{ss}$), with natural organic
 156 matter present in cloud sample, we used the formation rate of TAOH (Rf_{TAOH}) to calculate the
 157 steady state hydroxyl radical concentrations as follows:

$$158 \frac{d[TAOH]}{\gamma_{TAOH} dt} = k_{TA} \cdot [TA] \cdot [\bullet\text{OH}]_{ss} \quad (1)$$

159 So the steady state hydroxyl radical concentration can be calculated as follows:

$$160 [\bullet\text{OH}]_{ss} = \frac{d[TAOH]}{\gamma_{TAOH} \cdot k_{TA} \cdot [TA]} \quad (2)$$

161 To determine the steady state concentration, the linear part of the curve between Rf_{TAOH} and
 162 [TA] is used (Fig. S3). In fact, these conditions represent a low concentration of the probe in
 163 order to take into account the impact of all the natural scavengers present in cloud aqueous
 164 phase. The slope of the linear part of the equation is then divided by the second-order rate
 165 constant between TA and $\bullet\text{OH}$ (k_{TA}) and by the TAOH formation yield (γ_{TAOH}) as described in
 166 equation 2. These experimental conditions enable the determination of the real steady state
 167 concentration by taking into account the impact of all the chemical compounds present in the
 168 environment. Moreover, the use of TA as probe and the formation of TAOH which is detected
 169 by fluorescence spectroscopy, allows for reaching concentrations of $\bullet\text{OH}$ in the order of tenth
 170 of femtomolar.

171 For blank determination 8 measures have been performed in the dark. Limit of detection was
172 calculated as $\text{mean}_{\text{blank}} + 3\text{SD}_{\text{blank}}$ whereas LOQ was determined as $\text{mean}_{\text{blank}} + 10\text{SD}_{\text{blank}}$.
173 All the experimental and calculation details are presented in the supplementary data file
174 (Diagram S1, Fig. S1, S2, S3). Note that DMSO is used in order to stop the generation of
175 TAOH during the experiments through light irradiation and/or different chemical processes
176 occurring, thanks to its high reactivity with $\bullet\text{OH}$ ($k_{\text{DMSO}} = 6.6 \cdot 10^9 \text{ M}^{-1} \text{ s}^{-1}$) (Buxton et al.,
177 1988). The addition of 5 μL of DMSO (1 mM) immediately after the sampling does not
178 change significantly the quantification of $\bullet\text{OH}$ (Fig. S4).
179 Finally we tested this protocol to measure OH radical concentrations at the steady state in
180 controlled conditions using a microcosm mimicking cloud water conditions (artificial marine
181 cloud medium, artificial light, H_2O_2 and Fe-EDDS (ethylenediamine-N,N'-disuccinic acid)
182 complex as a source of radicals). The results are reported in the Supplementary Data (Figures
183 S5 and S6).

184 Wilcoxon test for paired data statistical analysis are performed on hydroxyl radical
185 concentration values to see significant difference (R software 3.5.0 used with $\alpha = 5\%$).

186

187 2.5. *Measurement of hydrogen peroxide concentration*

188 H_2O_2 concentrations are measured using an accurate enzymatic fluorimetric assay with a 4-
189 hydroxy-phenylacetic acid that produces a fluorescent dimeric compound with hydrogen
190 peroxide. This method is described in detail in the paper of Vaïtilingom et al. (2013).

191

192 2.6. *Assessment of the probe non-toxicity*

193 The non-toxicity of TA to microorganisms was evaluated on *Pseudomonas graminis* 13b-3,
194 DQ512786 isolated from cloud water sampled at the puy de Dôme station. *Pseudomonas*
195 *graminis* 13b-3 is incubated in R2A medium at 17°C and 130 rpm. After one day of

196 incubation, 6 mL of the culture are centrifuged for 3 min at 12 500 rpm. Cells pellets are
197 washed with NaCl 0.8% and cloud artificial medium. Optical density (OD) is taken with a
198 spectrophotometer (at $\lambda = 575$ nm) to obtain cell concentrations that are equal to 10^6 cells mL⁻¹
199 ¹ corresponding to concentration 10 times higher than in natural cloud water. Incubations are
200 done in cloud artificial marine media mimic the typical cloud chemical composition deriving
201 from marine influence. The used concentrations are also ten times higher than those reported
202 in natural cloud water, in order to keep the same ratio between cell and organic compound
203 concentrations. In fact, it has been showed that, at constant ratio “cell concentration/degraded
204 chemical compound concentration” and in the range of concentrations investigated,
205 biodegradation rates are independent of the absolute cell and chemical concentrations
206 (Vařtilingom et al., 2011): acetic acid 2.0×10^{-4} M, formic acid 1.45×10^{-4} M, oxalic acid
207 3.0×10^{-5} M, succinic acid 1.5×10^{-5} M, MgCl₂·6H₂O 1.0×10^{-4} M, CaCl₂·2H₂O 4.0×10^{-4}
208 M, K₂SO₄ 5.0×10^{-5} M, NaCl 2.0×10^{-3} M, NO₃NH₄ 8.0×10^{-4} M, NaOH 1.1×10^{-3} M and
209 H₂SO₄ 3.15×10^{-4} M. pH solution is adjusted to 6.1 close to the average pH of natural clouds
210 representative of air mass from marine origin (Deguillaume et al., 2014). The solution is
211 sterilized with 0.22 μ m PES filter (Polyethersulfone, diameter 28 mm, membrane of type
212 16532-k, Sartorius Stedium biotech, Germany) and kept in the dark at 17°C.
213 After incubation of cells, the media is tested with different concentrations of TA. At 0, 47 and
214 72 min of incubation, culture is done in R2A plate incubated at 17°C and ATP concentration
215 is measured with an ATP Biomass kit HS, BioThema[©].

216

217 **3. Results**

218

219 *3.1. Validation of the non-toxicity of terephthalic acid*

220 In order to see the impact of microorganisms on hydroxyl radical concentration, it is crucial to
221 check the non-toxicity of our probe. *Pseudomonas graminis* 13b-3 isolated in cloud water at
222 the puy de Dôme station is chosen as a model strain because it is representative of the major
223 actors of the cloud microbiota and on which we had already a lot of information available.
224 First it belongs to the *Pseudomonas* genus which is widely present in puy-de-Dôme cloud
225 samples. From cultural experiments we found this genus in 60% of our samples (Vaïtilingom
226 et al., 2012) and metatranscriptomics data showed that *Pseudomonas* strains are among the
227 most active in cloud waters (Amato et al., 2017). In addition we choose the strain
228 *Pseudomonas graminis* 13-b3 as a model strain because we already studied its metabolism in
229 Vaïtilingom et al (2010, 2011), Husarova et al (2011) and Wirgot et al (2017).
230 This strain is incubated at a concentration of $1.5 \pm 0.3 \times 10^6$ cells.mL⁻¹ with 3 different
231 probe concentrations (0, 4 and 10 μM) in “artificial marine” cloud medium. The evolutions of
232 cell counts and of ATP concentrations as a function of time are presented in Fig. 3.
233 Whatever the TA concentration, the number of bacteria remains within the same order of
234 magnitude and so no impact of probe concentration is detectable. Similarly, no major change
235 in ATP concentrations is observed with time under all the tested conditions, ranging from
236 1.6 to 2.6×10^{-6} pmol.cell⁻¹ with a mean value of 2.0×10^{-6} pmol.cell⁻¹.
237 Wirgot et al (2017) showed that *Pseudomonas graminis* 13-b3 metabolism and particularly its
238 ATP content are very sensitive to environmental conditions. For instance the ATP
239 concentration was highly impacted by the presence of H₂O₂, therefore *Pseudomonas graminis*
240 13-b3 is a good model to evaluate the impact of our probe on ATP concentration. In the same
241 paper we showed that the results issued from the study of this model strain (a strong
242 correlation between H₂O₂ and ATP concentrations) was valid when 32 cloud samples were
243 considered, containing a very diverse biodiversity. In this sense *P. graminis* 13-b3 was a
244 pertinent model for all the cloud microbiota.

245 Therefore we can conclude from the results of the present study that terephthalic acid does not
246 impact *Pseudomonas graminis* 13-b3 viability and energy. In addition we expect that all the
247 microorganisms in cloud water behave in a similar way than our model strain concerning TA
248 toxicity.

249 Consequently, this probe can be used for measuring microorganism's impact on hydroxyl
250 radical concentration.

251

252 3.2. *Hydroxyl radical steady state concentration in atmospheric waters*

253 With this method, [$\bullet\text{OH}$]_{ss} was evaluated under irradiation (2 hours) in various natural
254 atmospheric waters, 5 rain waters and 5 cloud waters sampled in 2015 and 2016.
255 Characterization of these atmospheric waters (including meteorological, physicochemical and
256 biological parameters) and their retro-trajectories over 120 h are presented in supplementary
257 data (Tables S1 and S2, Fig.S5 and S6, respectively).

258 During the two hours of irradiation the concentrations of $\bullet\text{OH}$ are evaluated at different
259 sampling times. At the same time, hydrogen peroxide concentrations are followed and no
260 decrease of the concentration is observed (data not shown). The steady state hydroxyl radical
261 concentrations obtained in rain and cloud waters are shown in Fig. 4. The standard deviations
262 for steady state concentration are calculated from plots of $R_{f\text{-TAOH}}$ versus TA concentrations.

263 Measured hydroxyl radical concentrations for atmospheric waters range from 2.8×10^{-17} M
264 (in rain water) to 2.0×10^{-15} M (in cloud water). Steady state hydroxyl radical concentrations
265 in cloud waters are higher than in rain waters, with values in cloud water ranging from
266 2.6×10^{-16} to 2.0×10^{-15} M with a mean value of $(7.2 \pm 5.0) \times 10^{-16}$ M and values in rain
267 water ranging from 2.8×10^{-17} to 4.3×10^{-16} M with a mean value of $(1.6 \pm 1.5) \times 10^{-16}$ M.
268 Thus the value of [$\bullet\text{OH}$]_{ss} is more than four times higher in cloud waters than in rain waters.
269 On the contrary, no significant differences are observed between our 5 cloud samples or our 5

270 rain samples. Moreover, no real correlation is found between the main parameters (Fe, H₂O₂,
271 NO₃⁻ and TOC) and OH radical concentration. The only tendencies observed are for the rain
272 samples with the highest TOC concentrations where the calculated OH radical concentrations
273 are the lowest and for the cloud samples where the OH radical concentrations increase with
274 the increase of nitrate concentration. These tendencies support the fact that TOC is a major
275 sink for OH radicals in natural water (Arakaki et al., 2013) and nitrate/nitrite could be an
276 important photochemical source of OH radical in such medium (Kaur and Anastasio, 2017).
277 However, from our results, no major influence of the air mass origins of the studied clouds
278 and rains could be detected on [[•]OH]_{ss}, 5 samples are not enough and more samples should be
279 analyzed to really conclude on this point.

280 After assessing the concentration of hydroxyl radicals in real atmospheric waters, the same
281 experiments are performed with filtered waters in order to see if microorganisms can impact
282 [[•]OH]_{ss} (Fig. 4). Concentration of hydroxyl radicals without (filtered) or with (non-filtered)
283 microorganisms in rain waters show similar results except for two samples where
284 concentrations are higher with the presence of microorganisms (September 17th, 2015 and
285 September 15th, 2016). This observation is even more obvious with cloud waters.
286 Systematically, the steady state concentrations of [•]OH are higher with microorganisms than
287 without microflora. However the difference is not statistically significant (p-value = 0.81 for
288 rain waters and 0.06 for cloud waters, paired Wilcoxon test used), microorganism impact
289 seems to be low, but more data are needed to strengthen this observation.

290

291 **4. Atmospheric implications and Conclusion**

292 A convenient method has been developed for the determination of steady state hydroxyl
293 radical concentration in real atmospheric waters. Indeed, terephthalic acid (TA) used as a
294 probe is non-toxic for microorganisms and therefore allows working with natural samples and

295 to study the impact of the microflora. Moreover, TA is soluble in water and not volatile so the
296 experiments can be performed in open-air conditions that are essential to work on natural
297 samples with microorganisms. Finally another positive aspect is that because of the formation
298 of a fluorescent product (TAOH) on which basis to evaluate the concentration of $\bullet\text{OH}$, the
299 technique is very sensitive with a limit of quantification near 10^{-17} M and the measurement is
300 easy to perform and fast. So, the use of TA is a very sensitive probe allowing direct
301 assessment of the steady state concentration of hydroxyl radicals considering the sinks
302 naturally present in the sample; it is complementary to the evaluation of the hydroxyl radical
303 formation rates obtained in many previous studies (Faust and Allen (1993) in cloud; Nakatani
304 *et al.* (2007) in rain and river, and Bianco *et al.* (2015) in cloud water). This result is thus
305 important for atmospheric scientists as the steady state hydroxyl radical concentration is really
306 a crucial parameter corresponding to the oxidant capacity of cloud water and more generally
307 of the atmosphere.

308 In this study, the measured values of the steady state hydroxyl radical concentrations are
309 within the range of few 10^{-16} M with mean values found in cloud water of " 7.2 ± 5.0 " $\times 10^{-16}$
310 M and in rain water of " 1.6 ± 1.5 " $\times 10^{-16}$ M.

311 As we can see in the Figure 5, our values are close to those published in different studies from
312 cloud, rain and fog waters even though our average of steady state OH radical concentration
313 in rain waters is around 10 times lower than those evaluated by Arakaki *et al.* (1999) and
314 Albinet *et al.* (2010). This difference can be explained by the typology of the sampling sites.
315 Indeed, Clermont-Ferrand area is much smaller than Torino or Higashi-Hiroshima and so less
316 polluted area with less photochemical sources of OH radical. This is confirmed by the average
317 concentration of nitrate in rain water measured in each site; Torino: 2.05 mg L^{-1} , Higashi-
318 Hiroshima 1.86 mg L^{-1} and Clermont-Ferrand 0.68 mg L^{-1} . On the other hand, our $[\bullet\text{OH}]_{\text{ss}}$

319 values found in cloud waters are within the same range than those measured by Anastasio and
320 McGregor (2001) in cloud waters and by Kaur and Anastasio (2017) in fog waters.

321 If we compare our mean values, the steady state hydroxyl radical concentration is four times
322 higher in cloud water than in rain water. This higher concentration in cloud water can be also
323 explained considering a higher concentration of photochemical sources of hydroxyl radicals in
324 cloud than in rain waters (Lin and Peng, 1999). For example, our average concentrations of
325 nitrate are 11.06 mg L^{-1} in cloud water and 0.68 mg L^{-1} in rain water.

326 Our results and comparison with the other studies show that nitrate (nitrite) could be the major
327 precursors for photoformed $\bullet\text{OH}$ in rain and cloud waters. This observation is in agreement
328 with the results published in the paper of Kaur and Anastasio (2017) which found that
329 nitrate/nitrite ions are responsible for 70% of photoformed $\bullet\text{OH}$ in fog waters. In contrast, the
330 study of Bianco et al. (2015) concluded that hydrogen peroxide is the most significant source
331 of this radical (between 70 and 90%) in cloud waters sampled at the the puy de Dôme station.
332 This discrepancy could be due to the origin of the air masses (continental, marine, polluted),
333 but also to the different kind of water fog or cloud and so the physicochemical properties of
334 the collected water which can drive the photochemical reactivity. In the study of Bianco et al.
335 (2015) no polluted samples was analysed and the puy de Dôme station in a remote site from
336 sources of pollution.

337 On the contrary, our values are much lower than most of the values estimated by cloud
338 chemistry models. Depending on the chemical scenarios (emission/deposition rates and initial
339 chemical conditions) and on the chemical mechanisms, the estimated $\bullet\text{OH}$ concentrations
340 vary from 10^{-12} M to 10^{-15} M (Deguillaume *et al.*, 2010; Herrmann *et al.*, 2010; Mouchel-
341 Vallon *et al.*, 2017; Tilgner and Herrmann, 2010; Tilgner *et al.*, 2013). The highest
342 concentration measured in the present study ($\sim 10^{-15} \text{ M}$) is close to the minimal value
343 simulated by the cloud chemistry models. This demonstrates that the models tend to

344 overestimate the hydroxyl radical concentration as previously mentioned by Arakaki *et al.*
345 (2013). This can be explained by two reasons. First, the models are expected to underestimate
346 the radical sinks because all the organic scavengers cannot be exhaustively considered in the
347 aqueous chemical mechanism. Secondly, models are simulating the mass transfer of $\bullet\text{OH}$
348 from the gas to the aqueous phase and consequently take into account an additional source not
349 considered in the present study. This additional source is estimated to represent 69% of the
350 total OH radical concentration present in aqueous phase (Kaur and Anastasio, 2017).

351 Moreover, thanks to this useful method, we have shown that the endogenous microflora has
352 no significant impact on the steady state hydroxyl radical concentrations. The microorganisms
353 could be a sink of $\bullet\text{OH}$ radicals as any other organic matter present in clouds; however this
354 quenching effect is suspected to be negligible as microorganisms represent a low fraction of
355 the total organic carbon (evaluated to 1.7% by Bauer *et al.*, 2002). On the contrary they could
356 produce $\bullet\text{OH}$ radicals by a passive mechanism. Indeed Samake *et al.* (2017) have recently
357 reported that dead microorganisms used as bioaerosol models (bacteria and fungi) can
358 produce ROS, although the method used does not allow to identify the type of radicals
359 formed. Finally our results can be interpreted in two ways: i) the production or quenching of
360 $\bullet\text{OH}$ is too low due to the low concentration of microorganisms in clouds thus no change in
361 $[\bullet\text{OH}]_{\text{ss}}$ can be measured; ii) the rates of production and consumption of $\bullet\text{OH}$ by
362 microorganisms are not negligible but within the same range of order and thus the resulting
363 $[\bullet\text{OH}]_{\text{ss}}$ remains constant.

364 This convenient tool will allow the evaluation of atmospheric water oxidant capacity; it
365 should be applied now to measure numerous samples at different sites (various altitudes,
366 latitudes, seasons, *etc.*). The $\bullet\text{OH}$ concentrations at the steady state will be used to evaluate
367 and constrain cloud chemistry models that simulate the organic matter transformations in
368 clouds and thus their composition, their evolution and lifetime. This will help to better assess

369 the effect of cloud of the transformation of atmospheric organic matter that plays a crucial
370 role on air quality and climate.

371

372 **Acknowledgements**

373 This work was funded by the French ANR program BIOCAP (N° ANR-13-BS06-004-01). It
374 was also supported by the French Ministry and CNRS. The authors acknowledge the financial
375 support from the Observatoire de Physique du Globe de Clermont-Ferrand (OPGC) and from
376 the Fédération des Recherches en Environnement through the CPER founded by Région
377 Auvergne Rhône-Alpes, the French ministry, and FEDER from the European community

378

379 **REFERENCES**

- 380 Albinet, A., Minero, C., and Vione, D., 2010. Photochemical generation of reactive species
381 upon irradiation of rainwater: Negligible photoactivity of dissolved organic matter. *Sci. Total*
382 *Environ.* 408, 3367–3373.
- 383 Amato, P., Parazols, M., Sancelme, M., Laj, P., Mailhot, G., and Delort, A.-M., 2007a.
384 Microorganisms isolated from the water phase of tropospheric clouds at the puy de Dôme:
385 major groups and growth abilities at low temperatures. *FEMS Microbiol. Ecol.* 59, 242–254.
- 386 Amato, P., Demeer, F., Melaouhi, A., Fontanella, S., Martin-Biesse, A.-S., Sancelme, M., Laj,
387 P., and Delort, A.-M., 2007b. A fate for organic acids, formaldehyde and methanol in cloud
388 water: Their biotransformation by micro-organisms. *Atmos. Chem. Phys.* 7, 4159–4169.
- 389 Anastasio, C., and McGregor, K.G., 2001. Chemistry of fog waters in California's Central
390 Valley: 1. In situ photoformation of hydroxyl radical and singlet molecular oxygen. *Atmos.*
391 *Environ.* 35, 1079–1089.
- 392 Arakaki, T., and Faust, B.C., 1998. Sources, sinks, and mechanisms of hydroxyl radical
393 ($\bullet\text{OH}$) photoproduction and consumption in authentic acidic continental cloud waters from
394 Whiteface Mountain, New York: The role of the Fe(r) (r = II, III) photochemical cycle. *J.*
395 *Geophys. Res.* 103, 3487–3504.
- 396 Arakaki, T., Miyake, T., Shibata, M., and Sakugawa, H., 1999. Photochemical formation and
397 scavenging of hydroxyl radical in rain and dew waters. *Nippon Kag. Kaish.* 5, 335–340.
- 398 Arakaki, T., Anastasio, C., Kuroki, Y., Nakajima, H., Okada, K., Kotani, Y., Handa, D.,
399 Azechi, S., Kimura, T., Tsuchioka, A., et al., 2013. A general scavenging rate constant for
400 reaction of hydroxyl radical with organic carbon in atmospheric waters. *Environ. Sci.*
401 *Technol.* 47, 8196–8203.
- 402 Ariya, P.A., Nepotchaykh, O., Ignatova, O., and Amyot, M., 2002. Microbiological
403 degradation of atmospheric organic compounds. *Geophys. Res. Lett.* 29, 34-1-34-4.

404 Bauer, H., Kasper-Giebl, A., Löflund, M., Giebl, H., Hitzemberger, R., Zibuschka, F., and
405 Puxbaum, H., 2002. The contribution of bacteria and fungal spores to the organic carbon
406 content of cloud water, precipitation and aerosols. *Atmos. Res.* 64, 109–119.

407 Bianco, A., Passananti, M., Perroux, H., Voyard, G., Mouchel-Vallon, C., Chaumerliac, N.,
408 Mailhot, G., Deguillaume, L., and Brigante, M., 2015. A better understanding of hydroxyl
409 radical photochemical sources in cloud waters collected at the puy de Dôme station –
410 experimental versus modelled formation rates. *Atmos. Chem. Phys.* 15, 9191–9202.

411 Bianco, A., Voyard, G., Deguillaume, L., Mailhot, G., and Brigante, M., 2016. Improving the
412 characterization of dissolved organic carbon in cloud water: Amino acids and their impact on
413 the oxidant capacity. *Sci. Rep.* 6.

414 Blough, N.V., and Zepp, R.G., 1995. Reactive oxygen species in natural waters. In *Active*
415 *Oxygen in Chemistry*, C. S. Foote, J. Valentine, A. Greenberg and J. F. Liebman (Springer),
416 pp. 280–330.

417 Brezonik, P.L., and Fulkerson-Brekken, J., 1998. Nitrate-induced photolysis in natural waters:
418 Controls on concentrations of hydroxyl radical photo-intermediates by natural scavenging
419 agents. *Environ. Sci. Technol.* 32, 3004–3010.

420 Buxton, G.V., Greenstock, C.L., Helman, W.P. and Ross, A.B., 1988. Critical review of rate
421 constants for reactions of hydrated electrons, hydrogen atoms and hydroxyl radicals ($\cdot\text{OH}/\text{O}^-$)
422 in aqueous solution. *J. Phys. Chem. Ref. Data* 17, 513–886.

423 Chameides, W.K., and Davis, D.D., 1982. The free radical chemistry of cloud droplets and its
424 impact upon the composition of rain. *J. Geophys. Res.* 87, 4863–4877.

425 Charbouillot, T., Brigante, M., Mailhot, G., Maddigapu, P.R., Minero, C., and Vione, D.,
426 2011. Performance and selectivity of the terephthalic acid probe for OH as a function of
427 temperature, pH and composition of atmospherically relevant aqueous media. *J. Photochem.*
428 *Photobiol. A* 222, 70–76.

429 Deguillaume, L., Leriche, M., Monod, A., and Chaumerliac, N., 2004. The role of transition
430 metal ions on HOx radicals in clouds: A numerical evaluation of its impact on multiphase
431 chemistry. *Atmos. Chem. Phys.* 4, 95–110.

432 Deguillaume, L., Leriche, M., and Chaumerliac, N., 2005. Impact of radical versus non-
433 radical pathway in the Fenton chemistry on the iron redox cycle in clouds. *Chemosphere* 60,
434 718–724.

435 Deguillaume, L., Desboeufs, K.V., Leriche, M., Long, Y., and Chaumerliac, N., 2010. Effect
436 of iron dissolution on cloud chemistry: From laboratory measurements to model results.
437 *Atmos. Poll. Res.* 1, 220–228.

438 Deguillaume, L., Charbouillot, T., Joly, M., Vaïtilingom, M., Parazols, M., Marinoni, A.,
439 Amato, P., Delort, A.-M., Vinatier, V., Flossmann, A., et al., 2014. Classification of clouds
440 sampled at the puy de Dôme (France) based on 10 yr of monitoring of their physicochemical
441 properties. *Atmos. Chem. Phys.* 14, 1485–1506.

442 Faust, B.C., 1994. Photochemistry of clouds, fogs, and aerosols. *Environ. Sci. Technol.* 28,
443 217A–222A.

444 Faust, B.C., and Allen, J.M., 1993. Aqueous-phase photochemical formation of hydroxyl
445 radical in authentic cloudwaters and fog waters. *Environ. Sci. Technol.* 27, 1221–1224.

446 Faust, B.C., and Hoigné, J., 1990. Photolysis of Fe (III)-hydroxy complexes as sources of OH
447 radicals in clouds, fog and rain. *Atmos. Environ.* 24, 79–89.

448 Faust, B.C., and Zepp, R.G., 1993. Photochemistry of aqueous iron (III)-polycarboxylate
449 complexes: Roles in the chemistry of atmospheric and surface waters. *Environ. Sci. Technol.*
450 27, 2517–2522.

451 Haag, W.R., and Hoigné, J., 1985. Photo-sensitized oxidation in natural water via OH
452 radicals. *Chemosphere* 14, 1659–1671.

453 Herckes, P., Valsaraj, K.T., and Collett, J.L., 2013. A review of observations of organic
454 matter in fogs and clouds: Origin, processing and fate. *Atmos. Res.* 132, 434–449.

455 Herrmann, H., Ervens, B., Jacobi, H.-W., Wolke, R., Nowacki, P., and Zellner, R., 2000.
456 CAPRAM2.3: A chemical aqueous phase radical mechanism for tropospheric chemistry.
457 *Journal of Atmospheric Chemistry* 36, 231–284.

458 Herrmann, H., Hoffmann, D., Schaefer, T., Brüner, P., and Tilgner, A., 2010. Tropospheric
459 aqueous-phase free-radical chemistry: Radical sources, spectra, reaction kinetics and
460 prediction tools. *ChemPhysChem* 11, 3796–3822.

461 Herrmann, H., Schaefer, T., Tilgner, A., Styler, S. A., Weller, C., Teich, M., Otto, T., 2015.
462 Tropospheric aqueous-phase chemistry: kinetics, mechanisms, and its coupling to a changing
463 gas phase. *Chem. Rev.* 115 (10), 4259–4334.

464 al Housari, F., Vione, D., Chiron, S., and Barbati, S., 2010. Reactive photo-induced species in
465 estuarine waters. Characterization of hydroxyl radical, singlet oxygen and dissolved organic
466 matter triplet state in natural oxidation processes. *Photochem. Photobiol. Sci.* 9, 78–86.

467 Husarova, S., Väitilingom, M., Deguillaume, L., Traïkia, M., Vinatier, V., Sancelme, M.,
468 Amato, P., Matulova, M., Delort, A.-M., 2011. Biotransformation of methanol and
469 formaldehyde by bacteria isolated from clouds. Comparison with radical chemistry. *Atmos.*
470 *Environ.* 45, 6093-6102.

471 Jacob, D.J., 1986. Chemistry of OH in remote clouds and its role in the production of formic
472 acid and peroxymonosulfate. *J. Geophys. Res.* 91, 9807–9826.

473 Joly, M., Amato, P., Sancelme, M., Vinatier, V., Abrantes, M., Deguillaume, L., and Delort,
474 A.-M., 2015. Survival of microbial isolates from clouds toward simulated atmospheric stress
475 factors. *Atmos. Environ.* 117, 92–98.

476 Kaur, R. and Anastasio, C., 2017. Light absorption and the photoformation of hydroxyl
477 radical and singlet oxygen in fog waters. *Atmos. Environ.*, 164, 387-397.

478 Lelieveld, J., and Crutzen, P.J., 1991. The role of clouds in tropospheric photochemistry. *J.*
479 *Atmos. Chem.* 12, 229–267.

480 Lelieveld, J., Dentener, F.J., Peters, W., and Krol, M.C., 2004. On the role of hydroxyl
481 radicals in the self-cleansing capacity of the troposphere. *Atmos. Chem. Phys.* 4, 2337–2344.

482 Lin, N.-H., and Peng, C.-M., 1999. Estimates of the contribution of below-cloud scavenging
483 to the pollutant loadings of rain in Taipei, Taiwan. *Terrestrial, Atmos. Ocean. Sci.* 10, 693–
484 704.

485 Mauldin III, R.L., Madronich, S., Flocke, S.J., and Eisele, F.L., 1997. New insights on OH:
486 measurements around and in clouds. *Geophys. Res. Lett.* 24, 3033–3036.

487 Metallo, C. M.; Vander Heiden, M. G., 2013. Understanding Metabolic Regulation and Its
488 Influence on Cell Physiology. *Mol. Cell.* 49 (3), 388–398.

489 Mill, T., Hendry, D.G., and Richardson, H., 1980. Free-radical oxidants in natural waters.
490 *Science* 207, 886–887.

491 Mouchel-Vallon, C., Deguillaume, L., Monod, A., Perroux, H., Rose, C., Ghigo, G., Long, Y.,
492 Leriche, M., Aumont, B., and Patryl, L., 2017. CLEPS 1.0: A new protocol for cloud aqueous
493 phase oxidation of VOC mechanisms. *Geosci. Model Dev.* 10, 1339–1362.

494 Nakatani, N., Ueda, M., Shindo, H., Takeda, K., and Sakugawa, H., 2007. Contribution of the
495 photo-Fenton reaction to hydroxyl radical formation rates in river and rain water samples.
496 *Anal. Sci.* 23, 1137–1142.

497 Page S.E., Arnold, W.A., McNeill K., 2010. Terephthalate as a probe for photochemically
498 generated hydroxyl radical. *J. Environ. Monit.* , 12, 1658-1665.

499 Parazols, M., Marinoni, A., Amato, P., Abida, O., Laj, P., Mailhot, G., Delort, A.-M., and
500 Sergio, Z., 2007. Speciation and role of iron in cloud droplets at the puy de Dôme station. *J.*
501 *Atmos. Chem.* 57, 299–300.

502 Qian, J., Mopper, K., and Kieber, D.J., 2001. Photochemical production of the hydroxyl
503 radical in Antarctic waters. *Deep Sea Res. Part I Oceanogr. Res. Pap.* 48, 741–759.

504 Russi, H., Kotzias, D., and Korte, F., 1982. Photoinduzierte hydroxylierungsreaktionen
505 organischer chemikalien in natürlichen Gewässern-Nitrate als potentielle OH-radikalquellen.
506 *Chemosphere* 11, 1041–1048.

507 Samake, A., Uzu, G., Martins, J.M.F., Calas, A., Vince, E., Parat, S., and Jaffrezo, J.L., 2017.
508 The unexpected role of bioaerosols in the oxidative potential of PM. *Sci. Rep.* 7.

509 Shingler, V., 2003. Integrated Regulation in Response to Aromatic Compounds: From Signal
510 Sensing to Attractive Behaviour. *Environ. Microbiol.* 5 (12), 1226–1241.

511 Tilgner, A., and Herrmann, H., 2010. Radical-driven carbonyl-to-acid conversion and acid
512 degradation in tropospheric aqueous systems studied by CAPRAM. *Atmos. Environ.* 44,
513 5415–5422.

514 Tilgner, A., Bräuer, P., Wolke, R., and Herrmann, H., 2013. Modelling multiphase chemistry
515 in deliquescent aerosols and clouds using CAPRAM3.0i. *J. Atmos. Chem.* 70, 221–256.

516 Tropel, D., van der Meer, J. R., 2004. Bacterial Transcriptional Regulators for Degradation
517 Pathways of Aromatic Compounds. *Microbiol. Mol. Biol. Rev.* 68 (3), 474–500.

518 Väitilingom, M., Amato, P., Sancelme, M., Laj, P., Leriche, M., and Delort, A.-M., 2010.
519 Contribution of microbial activity to carbon chemistry in clouds. *Appl. Environ. Microbiol.*
520 76, 23–29.

521 Väitilingom, M., Charbouillot, T., Deguillaume, L., Maisonobe, R., Parazols, M., Amato, P.,
522 Sancelme, M., and Delort, A.-M., 2011. Atmospheric chemistry of carboxylic acids:
523 Microbial implication versus photochemistry. *Atmos. Chem. Phys.* 11, 8721–8733.

524 Väitilingom, M., Attard, E., Gaiani, N., Sancelme, M., Deguillaume, L., Flossmann, A.I.,
525 Amato, P., and Delort, A.-M., 2012. Long-term features of cloud microbiology at the puy de
526 Dôme (France). *Atmos. Environ.* 56, 88–100.

527 Vaïtilingom, M., Deguillaume, L., Vinatier, V., Sancelme, M., Amato, P., Chaumerliac, N.,
528 and Delort, A.-M., 2013. Potential impact of microbial activity on the oxidant capacity and
529 organic carbon budget in clouds. *Proc. Natl. Acad. Sci.* 110, 559–564.

530 Weschler, C.J., Mandich, M.L., and Graedel, T.E., 1986. Speciation, photosensitivity and
531 reactions of transition metal ions in atmospheric droplets. *J. Geophys. Res.* 91, 5189–5204.

532 Wirgot, N., Vinatier, V., Deguillaume, L., Sancelme, M., Delort, A.-M., 2017. H₂O₂
533 modulates the energetic metabolism of the cloud microbiome. *Atmos. Chem. Phys.* 17,
534 14841-14851.

535 Yu, X.-Y., and Barker, J.R., 2003. Hydrogen peroxide photolysis in acidic aqueous solutions
536 containing chloride ions. I. Chemical mechanism. *J. Phys. Chem. A* 107, 1313–1324.

537 Zafiriou, O.C., and Bonneau, R., 1987. Wavelength-dependent quantum yield of OH radical
538 formation from photolysis of nitrite ion in water. *Photochem. Photobiol.* 45, 723–727.

539 Zellner, R., Exner, M., and Herrmann, H., 1990. Absolute OH quantum yields in the laser
540 photolysis of nitrate, nitrite and dissolved H₂O₂ at 308 and 351 nm in the temperature. *Atmos.*
541 *Chem.* 10, 411–425.

542 Zepp, R.G., Hoigne, J., and Bader, H., 1987. Nitrate-induced photooxidation of trace organic
543 chemicals in water. *Environ. Sci. Technol.* 21, 443–450.

544 Zhou, X., and Mopper, K., 1990. Determination of photochemically produced hydroxyl
545 radicals in seawater and freshwater. *Mar. Chem.* 30, 71–88.

546 **Figure captions:**

547 **Fig. 1:** Comparison of actinic fluxes of the lamp used in the present work together with the ones
548 measured under natural conditions during cloudy and sunny situations at the puy de Dôme station
549 (Solar emission in cloudy condition was measured in October 16th, 2013 and in sunny condition in
550 September 23th, 2013). Black line represents the lamp actinic flux, blue line is the actinic flux
551 measured under cloudy condition and red line is the actinic flux measured under sunny condition.
552 Dotted lines represent molar absorption coefficient ($M^{-1} cm^{-1}$) for Fe-EDDS complex (pink) and for
553 H_2O_2 (green).

554

555 **Fig. 2:** Reaction between TA and $\bullet OH$.

556

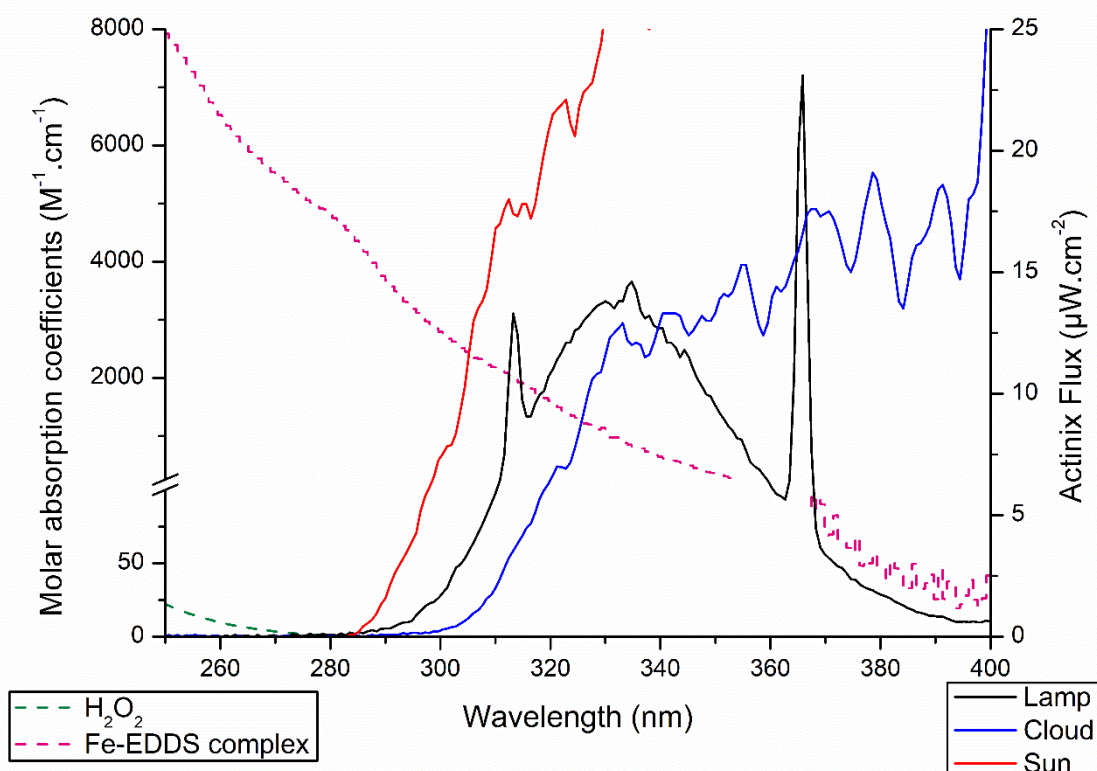
557 **Fig. 3:** Evolutions of the number of cells (A) and of the concentration of ATP (B) as a function of time
558 (0, 47 and 72 min) in the presence of 3 probe concentrations (0, 4 and 10 μM).

559

560 **Fig. 4:** Concentrations of hydroxyl radicals at steady state in rain and cloud waters without (white
561 histogram) and with microorganisms (dash histogram). Error bars represent standard variation from
562 plots of Rf_{TAOH} versus TA concentrations.

563

564 **Fig 5:** Measured of steady state hydroxyl radical concentrations by different research groups in
565 different atmospheric waters (cloud, fog and rain).

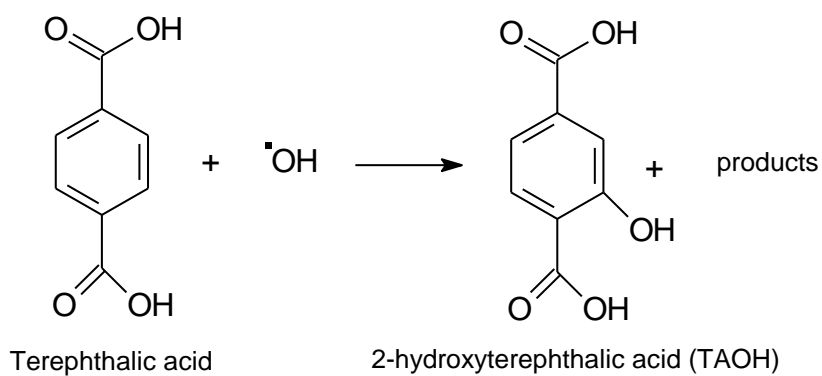


567

568 **Fig. 1**

569

570



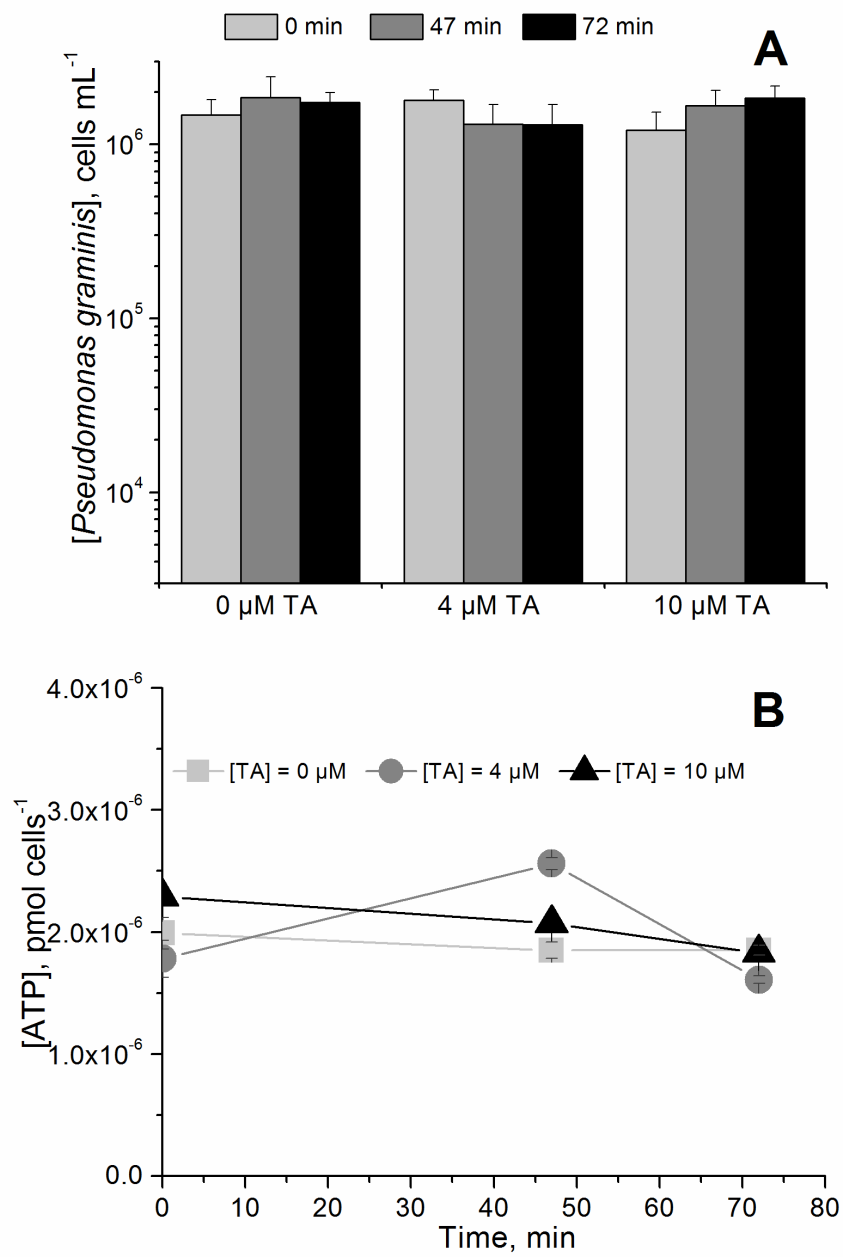
571

572

573 **Fig. 2**

574

575



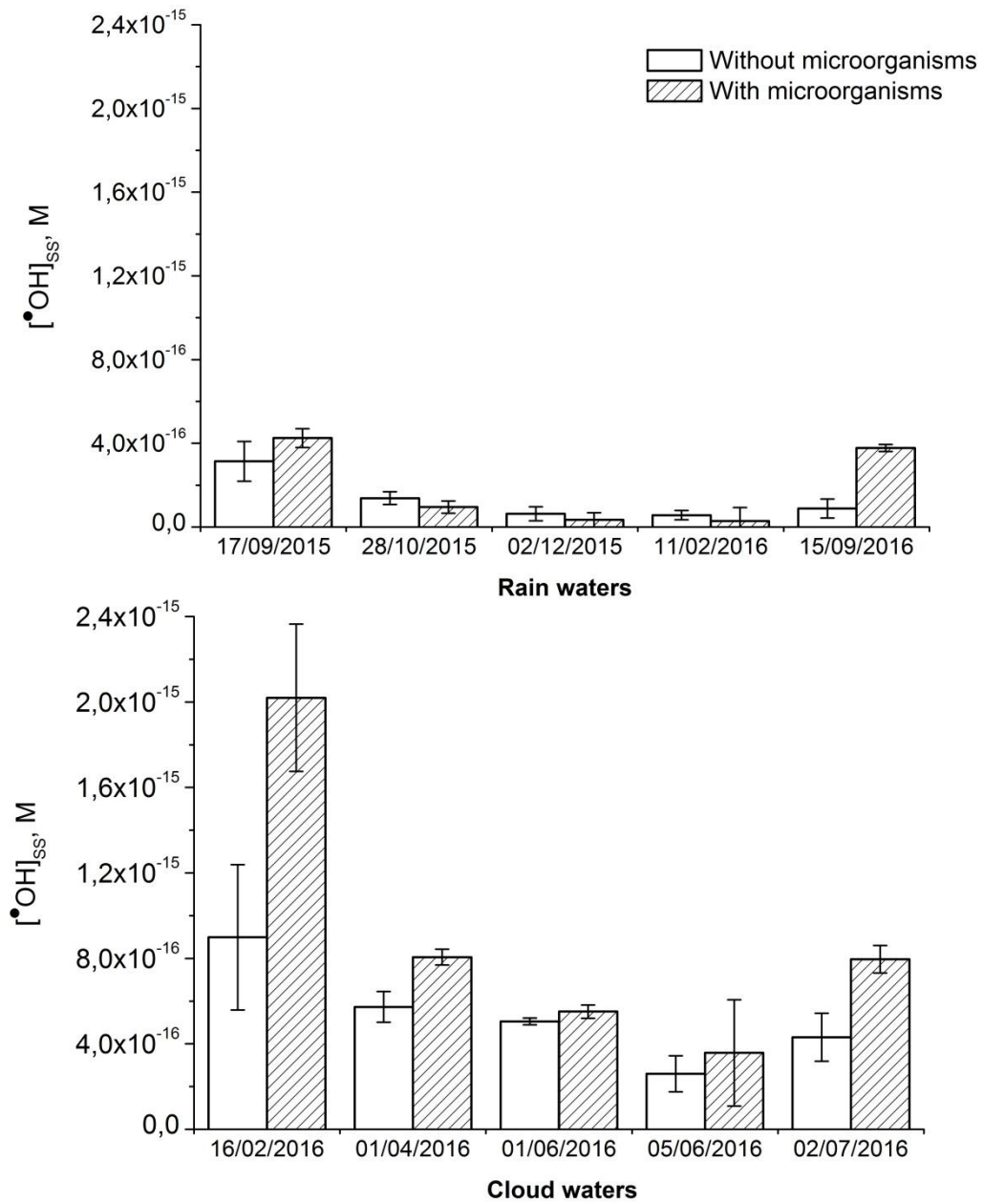
577

578 **Fig. 3**

579

580

581



582

583 **Fig. 4**

584

585

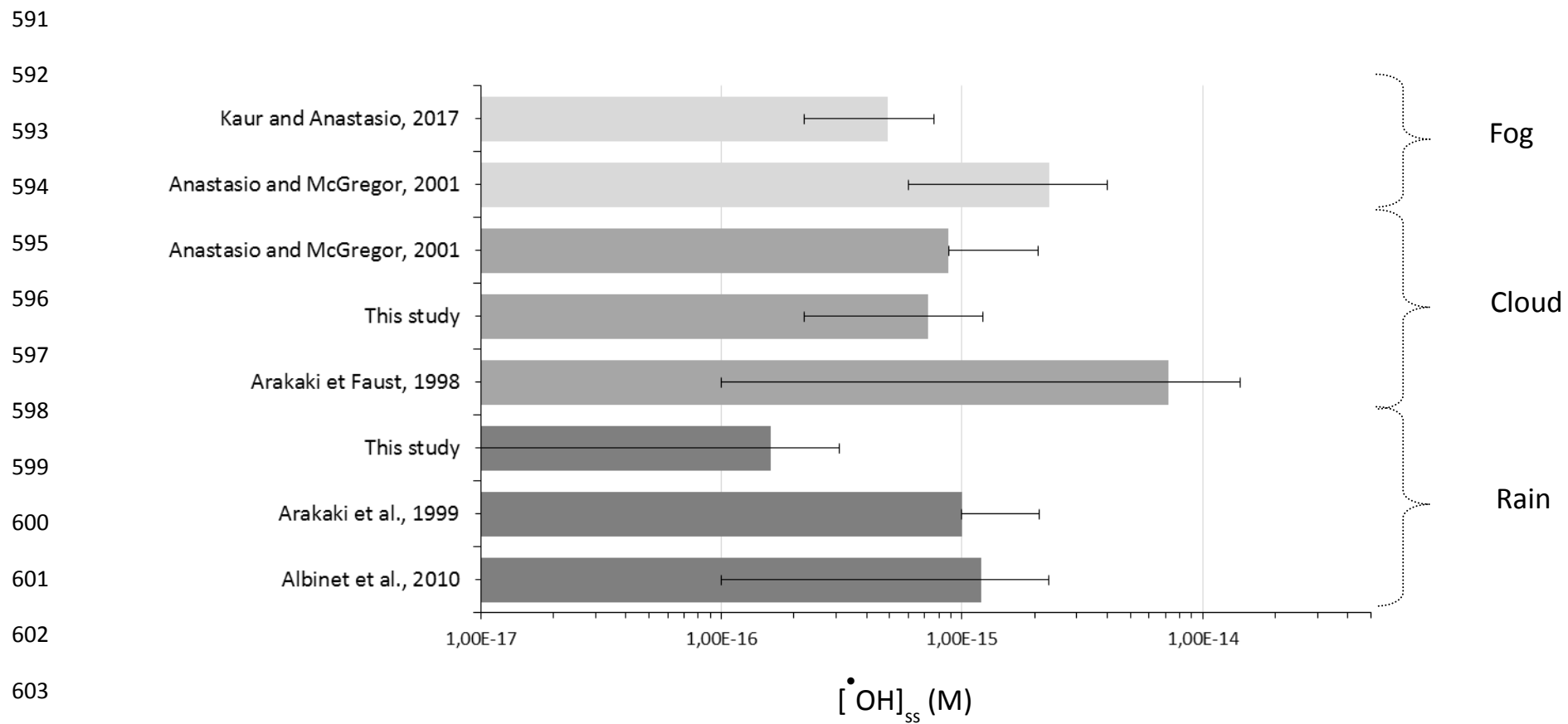
586

587

588

589

590



605 **Fig 5**